MEDWIN PUBLISHERS
Committed to Create Value for Researchers

Virology & Immunology Journal
ISSN: 2577-4379

In Silico Study by Quantum MicroRNA Language for the Development of Anti-COVID-19 Agents: COVID-19 Is Prevented by Rice MIR2097-5p through Suppression of SARS-Cov-2 Viral MicroRNAs plus HIPK2 Target Proteins

Fujii YR*

Kawada-Cho, 106-6, Atsuta-Ku, Nagoya, Japan

***Corresponding author:** Yoichi Robertus Fujii, Kawada-Cho, 106-6, Atsuta-Ku, Nagoya, Japan, Tel: 81526827003, Email: fatfuji@hotmail.co.jp

Research Article

Volume 4 Issue 4

Received Date: October 29, 2020

Published Date: November 19, 2020

DOI: 10.23880/vij-16000256

Abstract

Objective: The pandemic of coronavirus disease 2019 (COVID-19) is caused by severe respiratory syndrome human coronavirus 2 (SARS-CoV-2). We have previously found that mutations in haplotype C79F upon MAVS/VISA in Caucasian-American and African-American were fatal to COVID-19 compared to Asian-American in the USA model (approximate 100 times to Asian), which showed that there is a risk factor of people in Europa/America. This result was simulated by the integrated network algorithm as the MicroRNA (miRNA) entangling sorter (METS) analysis with quantum miRNA language. Since SARS-CoV-2 replication has been blocked *in vitro* and in patients by Honeysuckle, traditional Chinese herbal medicine, MIR2911, it was further investigated *in silico* that Japanese people might have some advantages into their culture against COVID-19 for prevention of SARS-CoV-2.

Materials and Methods: The METS computer analysis was performed as previously described. Information about coronavirus and miRNAs was extracted from the Viral Genomes and miRBase databases, respectively. The binding affinity between SARS-CoV-2 miRNAs and their targets was computed by mfold analysis. Sequence homology analysis among honeysuckle MIR2911 and other miRNAs was performed by BLASTN database.

Results and Discussion: The sequences of rice osa-MIR2097-5p was 52% homologous to those of MIR2911 and both plant miRNAs had similar properties in the quantum miRNA language. MIR2097-5p showed binding activity to SARS-CoV-2 viral miRNAs derived from the orf10 region and the 3' untranslated region (3'UTR) of the SARS-CoV-2 genome. Since MIR2097-5p simultaneously inhibited human homeodomain-interacting protein kinase 2 (HIPK2) protein target *in silico*, the expression of hypoxia inducible factor 1 subunit α (HIF1A) increased via viral miRNA and HIPK2 suppression by computer simulation with METS analysis. In addition, MIR2097-5p showed high affinity for 11 SARS-CoV-2 genome sites, including the 5'UTR. As a result, MIR2097-5p would prevent viral proliferation, and serious symptoms of COVID-19 could be remedied by MIR2097-5p. Since in Japan, both the number of patients and that of deaths per million people are much lower than USA, approximate 1/33 and 1/50, respectively. There are significant differences in the geographic distribution of infected patients between Asia and Europa/America. The cause of this regional difference in the number of patients and deaths per million people in Japan and USA may be due to the staple rice diet in Japan.

Conclusion: Thus, we found plant MIR2097-5p, a candidate for a 'quantum miRNA agent' against COVID-19.

Keywords: COVID-19; SARS-Cov-2; Plant; MicroRNA; Computer Simulation; *In silico*

Introduction

Significant differences of infection cases and deaths per million population of severe respiratory syndrome human coronavirus 2 (SARS-CoV-2) have been observed between Asia and Europa/America. For instance, in Japan, both the number of patients and deaths per million people is much lower than USA, approximate 1/33 and 1/50, respectively. The cause of this regional difference remains obscure. There was a hypothesis about regional differences in infection cases and deaths per million population that Bacillus Calmette-Guérin (BCG) vaccination may protect against severe coronavirus disease 2019 (COVID-19) because national COVID-19 mortality was negatively correlated with BCG vaccination rates [1]. However, there is no longer a statistically significant negative correlation between BCG vaccination rates and COVID-19 mortality [2]. Regarding the mechanism of action of BCG, the protective effect induced by BCG injection has been reported to be due to trained innate immunity, and the MAVS/VISA-associated NOD2 protein was implicated in the protection of COVID-19 via BCG-trained immunity [3]. Our recent computer simulation strongly supports the NOD2-BCG hypothesis. However, since the C79F haplotype of MAVS/VISA on mitochondria was a fatal risk factor for COVID-19, the BCG hypothesis may not be expected to directly contribute to regional differences [4]. Because the protecting effects of BCG through NOD2 signaling depends on pathogenic polymorphisms of the downstream transducer MAVS/VISA for production of type I interferon (IFN) against SARS-CoV-2 RNA. In addition, the mechanism of trained immunity remains unclear. We found 'the quantum MicroRNA immunity' as a programmed algorithm for trained immunity [5]. MAVS/VISA activity was enhanced by upregulation of HAUS augmin like complex subunit 8 (HAUS8), through programmed regulation of host miRNAs after SARS-CoV-2 invasion [6]. Therefore, the pathogenicity of COVID-19 could be usually regulated by the host miRNA, and SARS-CoV-2 RNA was defensed by the quantum miRNA immunity. Conversely, SARS-CoV-2 viral miRNAs targeted host proteins that were targeted by host miRNA, disrupting the host defense system and evading host defense mechanisms [4]. Thus, it suggested that the regional divergences in infected cases and deaths per million people would be due to the balance between defense upon the quantum miRNA immunity and evading by SARS-CoV-2 virus miRNA.

When considering plants as an industrial source of sustainable anti-virus agents, it is well known that Hippocrates has the wonderful phrase 'Let food be thy medicine and medicine be thy food' or a Chinese maxim, 'Food and medicine cognate' [7]. For example, rice bran is used in various vegetable pickles in Japan, but rice bran is wasted in many countries. In clinical food intervention trial in Nicaragua and Mali, rice bran has reduced diarrhea and improved environmental bowel dysfunction in children [8]. Given exogenous miRNAs derived from various food cultures, staple diets of Asia and Europa/America are rice and beef, respectively. Rice consuming countries locate in Asia, such as Japan, South Korea, China, Indonesia and India (fao.org/3/t0567e/T0567E04.htm). We have already mentioned in 'the RNA wave 2000' criteria that MicroRNAs (miRNAs) as mobile genetic elements move between cells and into cells, organs, or species to the environment [9]. We have reviewed that the idea of miRNA in exosomes can explain the absorption of exogenous milk miRNAs [7,10-12], and proposed the edible miRNA agents against human immunodeficiency virus type 1 (HIV-1). Therefore, it was hypothesized that the geographic difference in the number of patients infected with SARS-CoV-2 may be due to the difference between rice-based Japanese food and beef-based European dish. Because in Japan, South Korea and China, eating *Oryza sativa* Japonica rice as a daily diet showed significantly lower of COVID-19 cases and deaths in these countries than in USA about one each. It was approximate 1/33 and 1/50 in Japan vs USA, 1/50 and 1/100 in South Korea vs USA, and 1/500 and 1/200 in China vs USA (https://www.arcgis.com/apps/opsdashboard/index.html).

Rice *Oryza Sativa* Japonica (short rice) contains plant miRNAs, and the target proteins of plant miRNAs in plant cells have been predicted [13]. Plant miRNAs have regulated plant defense mechanisms against fungus rice-*Magnaporthe oryzae* [14] and plant RNA viruses, such as rice stripe virus (RSV) and rice dwarf virus (RDV) [15]. In addition, MIR2911-derived traditional Chinese herbal medicine Honeysuckle inhibited influenza A virus (H1N1)-encoded PB2 and NS1 protein expression and suppressed H1N1 viral replication [16]. Furthermore, the decoction honeysuckle MIR2911 was incorporated into the human circulatory system and blocked SARS-CoV-2 replication in infected patients [17]. Studies of the mechanism revealed that SID transmembrane family member 1 (SIDT1) in the gastric pit cell membrane mediates the uptake of dietary miRNAs into cells [18]. Zhou, et al. [19] also found that a human SIDT1 polymorphism (rs2271496) reduces the absorption of MIR2911 into human blood. These results about plant-derived miRNAs suggest that exogenous rice miRNAs might be absorbed and involved in human defense system against COVID-19.

We have previously showed *in silico* that the defense mechanism in viral infections, 'the quantum MicroRNA (miRNA) immunity' is programmed by the quantum miRNA language, but viruses produce viral miRNAs to evade the quantum miRNA immunity against SARS-CoV-2 infections [4-6]. Furthermore, by the miRNA entangling sorter (METS) simulation using quantum miRNA language, we have *in silico* simulated that vegetable-derived miRNAs could cure gastric cancer with *Helicobacter pylori* infection [20]. Vegetables and

Copyright© Fujii YR.

rice are extremely safe foods; therefore, food miRNAs, which is incorporated daily into the diet would be safer to use than traditional Chinese herb medicine without off-target effects or side effects on human illness. To prevent SARS-CoV-2 evading processes, we simulated the possibility of the quantum miRNA agent using plant miRNAs *in silico*.

Materials and Methods

Database Search

For extraction of rice data, Google Scholar (https://scholar.google.co.jp) and PubMed (www.ncbi.nlm.gov/pubmed/) were used. Total information content was 20,821 in rice food. The gene function of protein was searched by GeneCards (www.genecards.org). Protein ontology was investigated by GO enrichment analysis in Geneontology (geneontology.org). Data mining about rice miRNA was performed by homology search to honeysuckle MIR2911 [19]. Viral miRNAs and their target information were searched with VIRmiRNA (crdd.osdd.net/servers/virmirna/index.html).

METS Analysis for Plant miRNAs

METS analysis was performed by the computer processing as described previously [21,22]. The quantum energy of miRNA was calculated by double miRNAs' quantum energy levels of double nexus score (DNS) entangling single miRNA quantum energy levels of single nexus score (SNS). Data of multi-targets to a miRNA was extracted from TargetScan Human 7.2 (targetscan.org) and miRTarBase Ver. 8.0 (mirtarbase.cuhk.edu.cn). Target protein/protein interaction and protein cluster analysis were searched by STRING Ver. 11.0 (string-db.org). The area under the curve (AUC) in receiver operating characteristic (ROC), accuracy, precision and F values were calculated as previous description [22].

Functional Analogy Assay and Homology Analysis

Data of plant miRNA and viral genome was obtained from miR Base Ver. 22.1 (miRbase.org) and Viral Genomes (ncbi.nim.nih.gov). SARS-CoV-2 sequence (NC_045512.2) was used for calculation of binding ability with plant miRNA. The functional analogy assay between plant miRNA and human miRNA was performed as previously described [20]. BLASTN in miRBase was used for homology sequence search of miRNAs. The RNA secondary structure and the binding ability measuring of RNA were computed by mfold on RNA Folding Form (unafold.rna.albany.edu).

Results and Discussion

Homologous Plant miRNA to Honeysuckle MIR2911

Since the Honeysuckle MIR2911 (5'ggccgggggacggacuggga3') has been shown anti-SRAS-CoV-2 activity [19], analogy analysis with other miRNAs was primarily performed to investigate other plant miRNAs by homology sequence search. Twenty-eight miRNAs were hit with 52-64% sequence homology and three out of the 28 were selected as plant miRNAs, osa-miRNAs, osa-MIR1858a, osa-MIR1858b (5'gagaggaggacggagugggc3') and osa-MIR2097-5p (5'agagaugggacgggcagggaag3') (Table 1). Five human miRNAs, hsa-miR-6836-3p, hsa-miR-6834-5p, hsa-miR-6794-3p, hsa-miR-6748-5p and hsa-miR-4274, and bovine miRNA, bta-miR-11978, and two chicken miRNAs, gga-miR-6658-3p and gga-miR-1583 were selected as controls for the analysis below. A functional analogy assay between the honeysuckle MIR2911 and human miRNAs was done; however, hsa-miR-6836-3p, hsa-miR-6834-5p, hsa-miR-6794-3p, hsa-miR-6748-5p and hsa-miR-4274 did not show significant functional analogy in the seed region (data not shown).

ID	Homologous miRNA	MIR2911		Homologous miRNA		Direction	% homology	SNS
		Start	End	Start	End			
MIMAT0005541	**mcmv-miR-m22-1**	1	20	2	21	-	64	5
MIMAT0032315	**ssa-miR-128-2-5p**	1	20	4	23	+	64	11
MIMAT0050309	**mdo-miR-12371-3p**	1	18	3	20	+	63	10
MIMAT0015355	**zma-miR398b-5p**	7	20	1	14	+	61	10
MIMAT0021275	**mtr-miR5266**	3	19	1	17	+	58	11
MIMAT0007786	**osa-miR1858a**	5	19	5	19	+	57	12
MIMAT0007787	**osa-miR1858b**	5	19	5	19	+	57	13
MIMAT0012857	**rno-miR-678**	4	18	5	19	+	57	9
MIMAT0016906	**hsa-miR-4274**	3	17	4	18	-	57	3

Copyright© Fujii YR.

MIMAT0007444	**gga-miR-1583**	1	13	6	18	+	56	10
MIMAT0034505	**eca-miR-7045**	1	13	6	18	+	56	15
MIMAT0007002	**oan-miR-1360**	1	20	3	22	+	55	9
MIMAT0032316	**ssa-miR-128-3-5p**	1	20	4	23	+	55	12
MIMAT0044085	**gmo-miR-128-2-5p**	1	20	4	23	+	55	12
MIMAT0027782	**mmu-miR-6941-5p**	3	20	1	18	+	54	10
MIMAT0034722	**eca-miR-9146**	3	18	9	24	-	53	4
MIMAT0035102	**efu-miR-874**	1	16	9	24	+	53	8
MIMAT0040307	**pal-miR-874-3p**	1	16	9	24	+	53	9
MIMAT0005542	**mcmv-miR-M23-1-5p**	7	20	4	17	+	52	9
MIMAT0010058	**osa-miR2097-5p**	7	20	7	20	+	52	12
MIMAT0023672	**ame-miR-6048-3p**	5	18	9	22	+	52	11
MIMAT0025759	**gga-miR-6658-3p**	1	14	4	17	+	52	11
MIMAT0027396	**hsa-miR-6748-5p**	5	18	6	19	+	52	11
MIMAT0027489	**hsa-miR-6794-3p**	7	20	6	19	-	52	1
MIMAT0027568	**hsa-miR-6834-5p**	7	20	1	14	+	52	11
MIMAT0027575	**hsa-miR-6836-3p**	1	14	2	15	-	52	9
MIMAT0041839	**sfr-miR-10477-3p**	7	20	2	15	+	52	9
MIMAT0046364	**bta-miR-11978**	1	14	6	19	-	52	4

Table 1: Homologous miRNAs to MIR2911.

The plant miRNA sequence was then used to measure binding affinities to SARS-CoV-2 virus miRNA, Cov-miR-2 (5'uugucagaaugaauucucgu3'), Cov-miR-4 (5'guagauguaguuaacuuuaaucu3'), and Cov-miR-5 (5'uucaccgaggccacgcggaguacg3') with mfold (Table 2). The affinity for the pathogenic orf10 and the 3'untranslated region (UTR) was calculated. The mean initial free energy (ΔG: kcal/mol) between virus and rice miRNAs was obtained from each ΔG data. The top 2 average ΔG were osa-MIR2097-5p (-6.37) and hsa-miR-6748-5p (-7.67), and their free energies were approximately equivalent to MIR2911 (-7.25) (Table 2). Sequence analysis between rice and virus miRNAs revealed that the 5' terminal SARS-CoV-2 specific Cov-miR-2 seed and the osa-MIR2097-5p seed can pair with other's 3' sequences (Figure 1). MIR2911 had high affinity to Cov-miR-5 in 3'UTR only (Table 2 & Figure 1). As a positive search case, ΔG of artificial fragments that exactly match Cov-miR-2, Cov-miR-4 and Cov-miR-5 were calculated to be -28.8, -30.0 and -49.8, respectively. However, no plant and human miRNAs homologous to the exact matching artificial fragment were detected (data not shown). These data suggest that plant MIR2097-5p could specifically suppress pathogenic orf10 and 3'UTR activities *in silico* as anti-COVID-19 miRNA.

Anti-SARS-CoV-2 Candidate	**SARS-CoV-2 virus miRNA**			**Mean**
	orf10		**3'UTR**	
	Cov-miR-2	**Cov-miR-4**	**Cov-miR-5**	
MIR2911*	0.00**	0	-14.5	-7.25
osa-MIR2097-5p	**-9.6**	-2.8	-6.7	**-6.4**
osa-MIR1858a	-7.7	0	0	-2.57
hsa-miR-6836-3p	0	0	-12.3	-4.1
hsa-miR-6834-5p	-3.9	-4.1	-8.3	-5.43
hsa-miR-6794-3p	-0.9	0	-8.3	-3.07
hsa-miR-6748-5p	**-5.5**	-8	-9.5	**-7.7**

Copyright© Fujii YR.

hsa-miR-4274	0	0	-5.5	-1.83
bta-miR-11978	0	0	-13.5	-4.5
gga-miR-6658-3p	0	0	-6	-2
gga-miR-1583	0	0	-15.2	-5.07
Mean	-2.76	-1.35	-9.07	

Table 2: Exogenous miRNA targeting activity against virus miRNA.
*positive control, **initial free energy (ΔG). Bold: top two

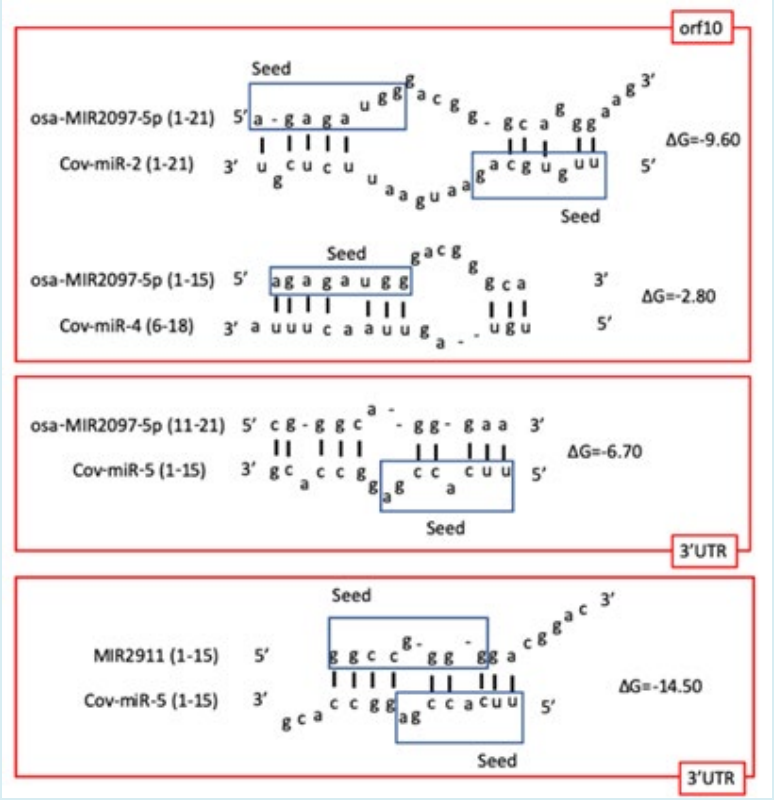

Figure 1: Plant miRNA targeting SARS-CoV-2 viral miRNAs. The targeting sequences of MIR2097-5p to viral miRNAs, Cov-miR-2 and Cov-miR-4 in orf10 (top panel), and Cov-miR-5 in 3'UTR (middle panel) were depicted. As a positive control, MIR2911 to Cov-miR-5 in 3'UTR was also depicted (bottom panel). The seed sequences were shown as blue square.

In silico Simulation of MIR2097-5p Activity against SARS-CoV-2 upon METS Analysis

Coherence with MIR2097-5p and SARS-CoV-2 virus miRNAs was firstly examined by METS computer simulation to investigate the virus-preventing effects of the plant miRNA. Rakhmetullina, et al. [23] has randomly predicted human target genes of rice miRNAs, but we used a functional analogy assay to predict MIR2097-5p targets. Data was extracted that the seed sequence of MIR2097-5p was homologous to those of hsa-miR-6858-5p. Twenty-three protein targets have been reported [23], and two proteins (Homeodomain-interacting protein kinase 2, HIPK2 and zinc finger protein 592, ZNF592) were extracted as the common molecules using a functional analogy assay (data not shown). HIPK2 only was associated with three COVID-19 etiological factors, infection, and neurodegeneration and lung disease. The MIR2097-5p had avidity for HIPK2 3'UTR position 1751-1757 at -13.0 ΔG. Since HIPK2 has inhibited HIF1A expression [24], plant MIR2097-5p with hsa-miR-147b-3p in *in silico* simulation upon METS analysis augmented HIF1A via suppression of HIPK2 as shown in Figure 2. About the difference of COVID-19 mortality between male and female (male>female), virus receptor angiotensin converting enzyme 2 (ACE2) expression has been induced via male steroids, and male HIPK2 haplotypes (rs2058265, rs6464214

Copyright© Fujii YR.

and rs7456421) were associated with higher systolic blood pressure [25,26]. Because higher blood pressure has been a risk factor of severe COVID-19 and hypertension was a risk factor independent from ACE2 expression in women [27], HIPK2 may be a risk factor of men distinctive from women. Therefore, suppression of HIPK2 by MIR2097-5p would be save people from COVID-19 due to hypertension. Simultaneously, MIR2097-5p suppressed Cov-miR-5 derived from the 3'UTR and increased HIF1A. These effects may suppress hypoxic pulmonary vascular hypertension of COVID-19. VIRmiRNA searches predicted that HIPK2 can be a target for Epstein-Barr virus (EBV) virus miRNAs, ebv-miR-BHRF1-2 and ebv-miR-BART18-5p. Thus, it is suggested that HIPK2 would be an important host molecule controlled by MIR2097-5p in the pathogenicity of COVID-19 lung.

Pathogenic Cov-miR-2 avidity for MIR2097-5p was higher than that for MAVS/VISA activity (ΔG; MIR2097-5p paired with Cov-miR-2 vs Cov-miR-2 paired with MAVS/VISA: -9.60 vs -8.40), that of complement C1QA and C1QB activities (-9.60 vs -6.10 and -9.60 vs -5.60), and that of acetylcholine esterase (ACHE) activity (-9.60 vs -6.10) (Figure 2). This indicates that SARS-CoV-2 specific pathogenicity by Cov-miR-2 was relevantly diminished by plant MIR2097-5p. Consequently, MIR2097-5p inhibited autonomic imbalance and lung inflammation, immunodeficiency, and virus production in *in silico* simulation using METS (Figure 2). These results in METS analysis were validated by the AUC values about viral infection, the AUC of MIR2097-5p plus was significantly decreased (AUC: 0.680) compared with that of viral miRNA alone (AUC: 0.947) (Table 3). These data showed that MIR2097-5p could reduce the effects of viral miRNAs in SARS-CoV-2 infection.

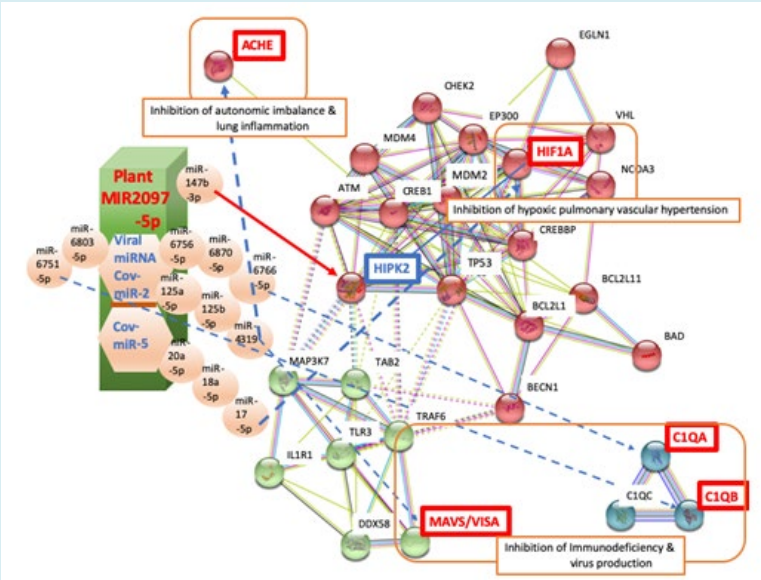

Figure 2: *In silico* simulation of the effects by MIR2097-5p against SARS-CoV-2 upon METS. The coherence with MIR2097-5p and SARS-CoV-2 viral miRNAs by METS simulation was presented. Suppressed host protein genes (ACHE, HIF1A, C1QA, C1QB and MAVS/VISA) through SARS-CoV-2 viral miRNA (Cov-miR-2 and Cov-miR-4) were recovered by plant MIR2097-5p. The COVID-19 symptoms are completely blocked as autonomic imbalance, lung inflammation, hypoxic pulmonary vascular hypertension, immunodeficiency and virus production. Red squared protein and red miRNA: upregulation, blue squared protein and blue miRNA: downregulation. Red arrow: suppressive effect. Blue bold and dotted line: disappeared effect.

	Virus infection	
	Viral miRNA alone	**Plant MIRNA plus**
AUC	0.947	0.68
Accuracy	0.955	0.85
Precision	0.964	0.9
F value	0.973	0.933

Table 3: Validation of *in silico* simulation with MIR2097-5p.

Translation Inhibition of SARS-CoV-2 by MIR2097-5p *in silico*

Host miRNAs have been reported to have binding affinities at various sites of SARS-CoV-2 genomic RNA [28], but miRNAs that bind to the orf10 region has not yet been reported. Therefore, this is the first report that plant miRNAs have the avidity to orf10 of the SARS-CoV-2 genome. Further, other MIR2097-5p binding sites in the SARS-CoV-2 genome were searched at the T1-T28 sites, which have revealed as

Copyright© Fujii YR.

the MIR2911 binding site [19]. Eleven sites of T1 in 5'UTR, T2, T3, T12, T13, T14 and T19 in orfab, T23 and T24 in S, T25 in E and T26 in M were identified with very high levels of free energy (Figure 3). The mean potentials of whole affinity (mean + SD) of MIR2097-5p and MIR2911 for the SARS-CoV-2 genome were -15.0 + 1.09 and -19.3 + 2.07, respectively (Figure 3). The MIR2097-5p putative binding site was broadly distributed in the viral genome. Although osa-MIR1858a did not show a significant average binding affinity for viral miRNAs (Table 2), possible binding sites of MIR1858a for the SARS-CoV-2 genome were found in T2, T3, T14 and T24. The free energies were ΔG -14.0, -18.2, -14.8 and -18.6, respectively. Seed paralogue hsa-miR-6858-5p showed similar binding affinities to the SARS-CoV-2 genome as osa-MIR2097-5p, except for T1 in 5'UTR and T12 in orfab (data not shown). The hsa-miR-6858-5p had Cov-miR-5 avidity in the 3'UTR (ΔG -15.4), but had no avidity to the Cov-miR-2 at all. These data suggest that suppression of Cov-miR-2 would be essential for effective prevention of SARS-CoV-2. In addition, osa-MIR2097-5p could affect SARS-CoV-2 RNA translation without off-target effects against human target proteins. On the other hand, when the viral miRNA Cov-miR-5 inhibited hsa-miR-6858-5p and the miR-6858-5p targeted HIPK2 3'UTR, so downregulation of miR-6858-5p derived from X chromosome (Xq28) would increase HIPK2; therefore, it could suppress HIF1A. This would cause severe COVID-19.

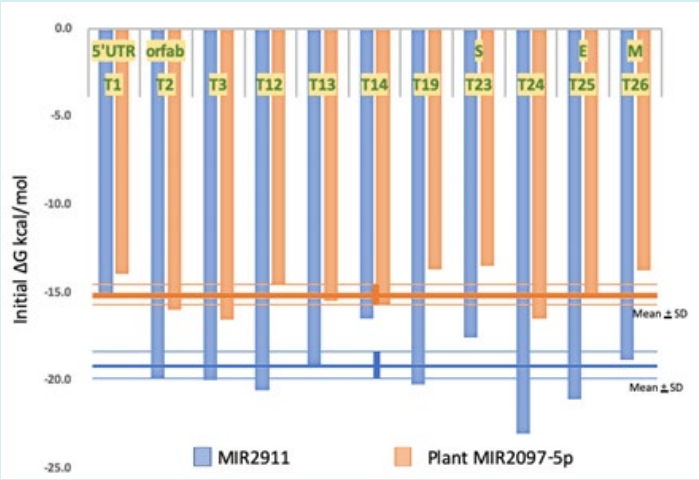

Figure 3: MIR2097-5p binding activities to the SARS-C-V-2 genome. Plant MIR2097-5p has the binding activity to the SARS-CoV-2 genome as T1 in 5'UTR, T2, T3, T12, T13, T14 and T19 in orfab, T23 and T24 in S, T25 in E, T26 in M sites (orange bars). As the control, the binding activities of honeysuckle MIR2911 were also presented (blue bars). The mean + SD of whole binding avidity in MIR2097-5p (orange lines) and MIR2911 (blue lines) was depicted as well.

MIR2911 binding activity to T1 to T28 sites (> -13.0) has already been confirmed by classical luciferase assays, and MIR2911 inhibited SARS-CoV-2 replication in both *in vitro* and infected patients [19]. In addition, it has been reported that when the nucleic acid mutual affinity is the highest, the biological activity is not high, and the optimum biological activity is obtained near the median value of the nucleic acid avidity activity [29]. Substantially, these results show that MIR2097-5p may inhibit translation of SRAS-CoV-2 proteins and viral replication more strongly than MIR2911. In Japan, younger people without smoking and anamnesis may not need the artificial COVID-19 vaccine to prevent COVID-19. Since rice miRNAs are contained in exosome, cooking and digestion have not significantly affected to exosome rice miRNAs [30]. Rice phyto-miRNA would then be absorbed via human SIDT1 and would affect host target proteins [31]. Therefore, the application of MIR2097-5p as a dietary supplement of 'food vaccine' may be able to reduce severe COVID-19 in the Europa and USA.

As a matter of constant debate, whether the effective amount of MIR2097-5p for viral prevention is relevantly presented in cells, Honeysuckle MIR2911 data showed that oral MIR2911 intake with Honeysuckle decoction (52.5 pM MIR2911 in 30g honeysuckle/200 ml decoction) was enough for antiviral effects. Only 13.2 pM MIR2911 completely inhibited virus replication *in vitro* and 0.42-1.13 pM MIR2911 in serum exosome inhibited SARS-CoV-2 replication in patients (2 hours after drinking) [19]. In Japan, people eat 119g rice/day/person and MIR2097-5p is very high abundant in rice [13]; therefore, it can be predicted that after 2 hours of diet, serum exosome would take up approximately 4 times the amount of MIR2097-5p and could inhibit viral replication. By daily uptake, phyto-miRNA has

Copyright© Fujii YR.

been accumulated in cells and circulatory systems, and reserved into long noncoding RNA (lncRNA) or circular RNA (circRNA), as miRNA memories, and has been maintained inside the cells for memory [7,32], albeit the viral miRNA memory with the same mechanisms would be also induced as the sequelae for a long term. Subsequently, the memory of phyto-miRNAs could continue to block that of viral miRNAs.

Participation of MIR2097-5p in the Geographic Difference of COVID-19 Cases and Deaths

Idogawa, et al. [33] have launched up a web site for COVID-19 cases and deaths per million people by country. According to the data on 22nd, October, 2020, the top 3 cases and deaths of COVID-19 were Brazil, USA and Argentina (Figure 4). Compared to USA (cases and deaths: 21725.1 and 622.3), in China, South Korea and Japan, the number of cases and deaths has been 62.9 and 3.3, 464.5 and 8.1, and 656.3 and 12.4, which is very low since the start date of the pandemic, 31st, December, 2019, respectively (Figure 4). Since we have already reported the risk factors of MAVS/VISA haplotype and mitochondria aging, it was predicted that, even after the bottleneck effect of MAVS/VISA polymorphism, further some advantages in the Japanese culture may cause the difference in COVID-19 cases and deaths per million people by country [4]. Although there are social distancing, face masking and shutdowns to control the spread of COVID-19, it is difficult to reach herd immunity through natural transmission. However, there is an evidence of the geographical difference in COVID-19 cases and deaths. Regarding food culture, it is well known that the Western diet is very distinct from the Japanese diet. According to 1984 FOOD and Agriculture Organization (FAO) data, rice milling availability in China, South Korea and Japan was 104, 98 and 64 kg/caput/year, respectively. In 1987-89 FAO data, the average daily energy intake of rice as staple food in China, South Korea and Japan was 2350, 2853 and 2909 kcal/caput/day, respectively. According to FAO data for 2014-15, rice consumption in China, South Korea and Japan was 1475000, 4450 and 7966 thousand tons, respectively, and the g/day/person consumption was 219, 234 and 119, respectively. The rice cooking area including Australia was at a low level of COVID-19 cases and deaths per million people. In addition, in Indonesia, rice *Oryza sativa* Indica (long rice) consumption was 364 g/day/person, with cases and deaths per million people slightly higher at 1033.6 and 38.8 (Figure 4). The number of cases and deaths in staple Japonica diet countries was lower than in Indica countries (Figure 4). It is suggested that Japonica may contain much more amounts of MIR2097-5p than Indica, or people in staple Indica diet countries may have a human SIDT1 polymorphism (rs2271496) and/or other pathogenic human gene polymorphisms, such as MAVS/VISA in their genomes. Thus, the data is strong evidence that rice food MIR2097-5p would be a possible blockade into the Japanese culture against COVID-19.

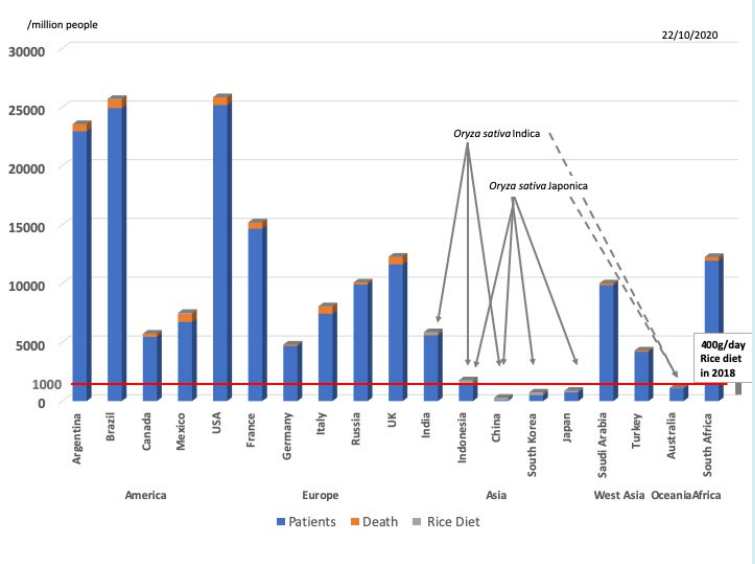

Figure 4: COVID-19 cases and deaths. COVID-19 cases (blue bars) and deaths (orange bars) /million population were presented among countries on 22nd, October, 2020. Rice diet consumption (g/day/person) (gray bars) among countries was integrated into COVID-19 cases and deaths. Rice contains *Oryza sativa* Japonica and *Oryza sativa* Indica. Right side gray bold line: the scale of 400g/day rice diet in 2018. Dotted lines: not staple diet of rice.

Copyright© Fujii YR.

Altogether, it is suggested that plant MIR2097-5p could be a 'quantum miRNA agent' candidate against SARS-CoV-2 (Figure 5), and those *in silico* results may strongly support that quite low levels of COVID-19 cases and deaths per million mass population are resulted in China, South Korea and Japan as rice consuming countries. There would be far more asymptomatic carriers per million in these regions than USA. Thus, from *in silico* our studies [4-6,34,35], the quantum MicroRNA language for METS is a beneficial computer algorithm for the development of quantum MicroRNA drugs, and the direction of future research for human diseases such as infectious diseases and cancers would be determined by such integrated algorithms. The construction of a computer system with artificial intelligence (AI), such as an AI doctor using quantum MicroRNA language, can provide appropriate incentives for the precious medicine and the development of therapeutic agents. Further investigations are needed.

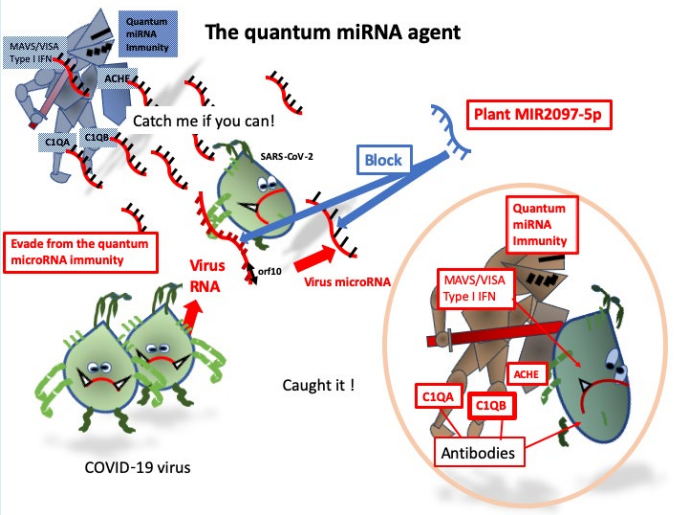

Figure 5: The quantum miRNA agent. We have the quantum miRNA immunity to protect viral infection as the first defense program. SARS-CoV-2 genomic RNA produces orf10 mRNA. The orf10 RNA produces viral miRNA, Cov-miR-2. Cov-miR-2 is quite pathogenic, which targets acetylcholine esterase (ACHE), complement C1QA and C1QB and MAVS/VISA type I interferon (IFN) producing pathway. SARS-CoV-2 evades from the quantum miRNA immunity [36,37]. Consequently, COVID-19 infected patients and deaths are increasing. Since plant miRNAs are absorbed into human cells and circulating system, incorporated miRNAs affect human proteins. Not only human proteins but also infected viral RNAs are downregulated by plant phyto-miRNA, such as honeysuckle MIR2911 against influenza virus, varicella-zoster virus and SARS-CoV-2. Plant MIR2097-5p could charge to SARS-CoV-2 Cov-miR-2 and genomic RNA, which can block COVID-19 viral production and its symptoms as shown in the METS network of Figure 2. 'RNA controls RNA' [36, 37]. In Japan, our staple diet is rice and COVID-19 cases and deaths are very low; therefore, MIR2097-5p is a 'the quantum miRNA agent' candidate to prevent COVID-19 infection.

Conclusion

Plant MIR2097-5p has binding strength to SARS-CoV-2 virus miRNAs (Cov-miR-2 and Cov-miR-5) and high affinity for the viral genome. From *in silico* computer simulation using METS, MIR2097-5p protected MAVS/VISA activity, C1QA and C1QB activities, and ACHE activity with downregulation of Cov-miR-2. Furthermore, HIPK2 suppression by MIR2097-5p inhibited hypoxic pulmonary vascular hypertension of COVID-19. In addition, plant MIR2097-5p prevented viral replication in *in silico* by preventing translation of viral proteins. MIR2097-5p in the staple rice diet was predicted to be a factor in country-to-country differences in SARS-CoV-2 infections and deaths per million population. Thus, I found plant MIR2097-5p as a 'quantum miRNA agent' candidate against SARS-CoV-2.

Conflicts of Interest

The authors declare that there are no conflicts of interest.

References

1. Jirjees FJ, Dallal Bashi YH, AI Obaidi HJ (2020) COVID-19 death and BCG vaccination programs worldwide. Tuberc Respir Dis. in press.

2. Lindestam Arlehamn CS, Sette A, Peters B (2020) Lack of evidence for BCG vaccine protection from severe COVID-19. Proc Natl Acad Sci USA 117(41): 25203-25204.

3. Wannigama DL, Jacquet A (2020) NOD2-dependent

Copyright© Fujii YR.

BCG-induced trained immunity: a way to regulate innate responses to SARS-CoV2?. Int J Infect Dis 101: 52-55.

4. Fujii YR (2020) The COVID-19 deadly risk assessment upon the updated etiologic computer simulation by quantum MicroRNA language in SARS-CoV-2 infection *in eo*. Int J Clin Case Stud Rep 3(1): 142-154.

5. Fujii YR (2020) The quantum MicroRNA immunity in human virus-associated diseases: virtual reality of HBV, HCV and HIV-1 infection, and hepatocellular carcinogenesis with AI machine learning. Arch Clin Biomed Res 4: 89-129.

6. Fujii YR (2020) The etiology of COVID-19 *in silico* by SARS-Cov-2 infection with the quantum MicroRNA language-AI. Virol Immunol J 4(2): 000243.

7. Fujii YR (2017) The MicroRNA 2000: from HIV-1 to healthcare. Scientific Research Publishing Inc Irvine, CA.

8. Zambrana LE, Mckeen S, Ibrahim H, Zarei I, Borresen EC, et al. (2019) Rice bran supplementation modulates growth, microbiota and metabolome in weaning infants: a clinical trial in Nicaragua and Mali. Sci Rep 9(1): 13919.

9. Fujii YR (2008) Formulation of new algorithmics for miRNAs. Open Virol J 2: 37-43.

10. Brisibe EA, Okada N, Mizukami H, Okuyama H, Fujii YR (2003) RNA interference: potentials for the prevention of HIV infections and the challenges ahead. Trends Biotechnol 21(7): 306-311.

11. Fujii YR (2008) Symphony of AIDS. In Rossi JJ, Gaur RK, (Eds.), Regulation of gene expression by small RNAs. CRC press Boca Raton FL pp: 333-349.

12. Fujii YR, Saksena NK (2008) Viral infection-related MicroRNAs. In: Morris KV (Eds.), Viral and host genomic evolution in RNA and the relation of gene expression. Horizon Scientific Press London UK pp: 91-107.

13. Xue LJ, Zhang JJ, Xue HW (2009) Characterization and expression profiles of miRNAs in rice seeds. Nucleic Acids Res 37(3): 916-930.

14. Li Y, Martin J, Jeyakumar J, Feng Q, Zhao ZX, et al. (2019) The roles of rice MicroRNAs in rice-*Magnaporthe oryzae* interaction. Pthytopath Res 1: 33.

15. Baldrich P, San Segundo B (2016) MicroRNAs in rice innate immunity. Rice 9: 6.

16. Zhou Z, Li X, Liu J, Dong L, Chen Q, et al. (2015) Honeysuckle-encoded atypical MicroRNA2911 directly targets influenza A viruses. Cell Res 25: 39-49.

17. Zhou Z, Zhou Y, Jiang XM, Wang Y, Chen X, et al. (2020) Decreased HD-MIR2911 absorption in human subjects with the SIDT1 polymorphism fails to inhibit SARS-CoV-2 replication. Cell Discovery 6: 63.

18. Chen Q, Zhang F, Dong L, Wu H, Xu J, et al. (2020) SIDT1-dependent absorption in the stomach mediates host uptake of dietary and orally administered MicroRNAs. Cell Res: 1-12.

19. Zhou LK, Zhou Z, Jiang XM, Zheng Y, Chen X, et al. (2020) Absorbed plant MIR2911 in honeysuckle decoction inhibits SARS-CoV-2 replication and accelerates the negative conversion of infected patients. Cell Discovery 6: 54.

20. Fujii YR (2019) Quantum MicroRNA network analysis in gastric and esophageal cancers: xenotropic plant MicroRNAs cure from cancerous paradox via *Helicobacter pylori* infection. Gastroenterol Hepatol Endosc 4: 1-18.

21. Fujii YR (2013) The RNA gene information: retroelement-MicroRNA entangling as the RNA quantum code. Methods Mol Biol 936: 47-67.

22. Fujii YR (2018) Quantum language of MicroRNA: application for new cancer therapeutic targets. Methods Mol Biol 1733: 145-157.

23. Rakhmetullina A, Pyrkova A, Aisina D, Ivashchenko A (2020) *In silico* prediction of human genes as potential targets for rice miRNAs. Comput Biol Chem 87: 107305.

24. Calzado MA, De La Vega L, Munoz E, Schmitz ML (2009) From top to bottom: the two faces of HIPK2 for regulation of the hypoxic response. Cell Cycle 8(11): 1659-1664.

25. Kalidhindi RSR, Borkar NA, Ambhore NS, Pabelick CM, Prakash YS, et al. (2020) Sex steroids skew ACE2 expression in human airway: a contributing factor to sex differences in COVID-19?. Am J Physiol Lung Cell Mol Physiol 319(5): 843-847.

26. Lin H, Zhu X, Long J, Chen Y, Xie Y, et al. (2018) HIPK2 polymorphisms rs2058265, rs6464214, and rs7456421 were associated with kidney stone disease in Chinese males not females. Gene 653: 51-56.

27. Rodilla E, Saura A, Jiménez I, Mendizábal A, Pineda-Cantero A, et al. (2020) Association of hypertension with all-cause mortality among hospitalized patients with COVID-19. J Clin Med 9(10): E3136.

28. Chow JT, Salmena L (2020) Prediction and analysis of SARS-CoV-2 targeting MicroRNA in human lung epithelium. Gene 11: 1002.

Copyright© Fujii YR.

29. Straarup EM, Fisker N, Hedtjárn M, Lindholm MW, Rosenbohm C, et al. (2010) Short locked nucleic acid antisense oligonucleotides potently reduce apolipoprotein B mRNA and serum cholesterol in mice and non-human primates. Nucleic Acids Res 38(20): 7100-7111.

30. Philip A, Ferro VA, Tate RJ (2015) Determination of the potential bioavailability of plant MicroRNAs using a simulated human digestion process. Mol Nut Food Res 59(10): 1962-1972.

31. Malloci M, Perdomo I, Veerasamy M, Andriantsitohaina R, Simard G, et al. (2018) Extracellular vesicles: mechanisms in human health and disease. Antioxid Redox Signal 30: 813-856.

32. Fujii YR (2018) The quantum language of the MicroRNA gene and anti-cancer: with a dynamic computer simulation of human breast cancer drug resistance. Int Mol Med 5: 1-23.

33. Idogawa M, Tange S, Nakase H, Tokino T (2020) Interactive Web-based graphs of coronavirus disease 2019 cases and deaths per population by country. Clin Infect Dis 71(15): 902-903.

34. Fujii YR (2019) Cancer simulation from stage minus one by quantum MicroRNA language: lung, colorectal and pancreatic cancers. Med One 4: e190023.

35. Osone T, Yoshikawa M, Fujii YR (2016) Quantum fluctuation in biological functions: computational analysis of diseases with the human MicroRNA memory package. SAI Comp Conf (SAI) 2016: 1206-1210.

36. Fujii YR (2020) COVID-19 Video FujiiYR. Virol Immunol J.

37. Fujii YR (2020) MicroRNA COVID STORY. Virol Immunol J.

Copyright© Fujii YR.